Наносистеми, наноматеріали, нанотехнології
Nanosistemi, Nanomateriali, Nanotehnologii
2026, т. 24, № 2, сс. 441–454
https://doi.org/10.15407/nnn.24.02.0441

PACS numbers: 68.37.Lp, 72.40.+w, 73.20.Mg, 78.40.-q, 78.55.-m, 81.16.Mk, 88.40.jp

Effect of Silver Nanoparticles on Solar Cell Efficiency: Size and Optical Characteristics *via* Pulsed Laser Ablation in Liquids and Laser Energies

N. G. Abed[1], S. M. Ahmad[1], and Th. A. Zaker[2,3]

[1]*College of Sciences,*
Department of Physics,
University of Mosul,
Nineveh, Iraq
[2]*College of Education,*
Department of Physics,
University of Al-Hamdaniya,
Nineveh, Iraq
[3]*Department of Laser and Spectroscopy,*
Laser and Photonics Center,
University of Al-Hamdaniya,
Nineveh, Iraq

Various applications make the use of silver nanoparticles (Ag NPs) due to their chemical durability, high light absorption, and superior conductivity. This research demonstrates that pulsed laser ablation with varying energy in a variety of liquids can produce Ag NPs. The effect of Ag NPs on the efficiency of solar cells is investigated. Nanocolloids' dimensions, forms, and absorption spectra are measured by ultraviolet–visible (UV–Vis) spectroscopy, photoluminescence (PL), and transmission electron microscopy (TEM). The distribution and mean diameter are investigated with the use of image-java tools. The results show that the best-characterized Ag NPs are made by combining the 1 Hz-pulse repetition rate with an acetone solution and the 1000 mJ-laser energy. These Ag NPs display the most uniform shape, narrowest size dispersion of 10–40 nm, and shortest mean diameter of 21.56 nm. The results of the Ag NPs' precipitation experiment on the solar cell show a 20% improvement in the cells' conversion efficiency.

Різні застосування використовують наночастинки срібла (Ag-НЧ) завдяки їхній хемічній стійкості, високому вбирання світла та чудовій провідності. Це дослідження демонструє, що імпульсна лазерна абляція з різною енергією у різних рідинах може утворювати Ag-НЧ. Було досліджено вплив Ag-НЧ на ефективність сонячних елементів. Розміри,

форми та спектри вбирання наноколоїдів було виміряно за допомогою спектроскопії ультрафіолетового-видимого випромінення, фотолюмінесценції та просвітлювальної електронної мікроскопії. Розподіл і середній діяметер досліджували за допомогою інструментів зображення-java. Результати показали, що найліпше охарактеризовані Ag-НЧ було одержано шляхом поєднання частоти повторення імпульсів у 1 Гц з розчином ацетону та лазерної енергії у 1000 мДж. Ці Ag-НЧ продемонстрували найбільш однорідну форму, найменшу дисперсію розмірів у 10–40 нм і найкоротший середній діяметер у 21,56 нм. Результати експерименту з осадження Ag-НЧ на сонячному елементі показали 20%-поліпшення ефективности трансформування елемента.

Key words: solar cell, Ag nanoparticles, colloids, laser ablation, plasmon resonance.

Ключові слова: сонячний елемент, наночастинки срібла, колоїди, лазерна абляція, плазмонний резонанс.

(Received 17 December, 2024; in revised form, 17 February, 2025)

1. INTRODUCTION

Silver nanoparticles (Ag NPs) are particularly advantageous for use in solar cells due to their unique plasmonic properties, which enhance light absorption and scattering. Compared to other conductive elements like gold or aluminium, silver offers a higher conductivity and better plasmonic response in the visible spectrum, making it more effective for improving solar cell efficiency. Additionally, Ag NPs are more cost-effective and chemically stable, which further supports their use in photovoltaic applications.

Solar cells are one of the most significant sources of clean energy because of the steadily rising need for renewable energy. Increasing the efficiency of conventional solar cells is still quite difficult [1]. Due to its low cost, natural availability, nontoxicity, long-term stability, and well-established technology, silicon (Si) is the material most frequently employed in photovoltaic applications. However, one of the challenges to increasing solar cell efficiency is its weak absorption [2, 3]. Anti-reflecting coating layers and texturing structures enhance silicon absorption; however, these require chemical treatment and expensive deposition techniques. Plasmonic effects from a noble metal nanoparticle can greatly increase the solar cells' ability to absorb light and, consequently, their conversion efficiency [1]. This is due to metals' high free-electrons' density [1] and can cause surface plasmon resonance (SPR) [2] due to their strong interactions with visible light. The shape, size, and surrounding dielectric medium of the metal nanoparticles mostly de-

termine the resonant oscillation of conduction electrons about the positive-ion core under proper light irradiation, which is known as the surface plasmon resonance [3, 4].

SPR features enhance and control light at the nanoscale, hence, improving the sensitivity and resolution of optical instruments. Plasmonic nanoparticles can either augment or diminish photocurrent in the device, contingent upon wavelength, nanoparticle resonance, and the size and geometry of the nanostructure [5]. Sunlight can be collected and confined by SPR, hence, enhancing absorption intensity [6]. Forward scattering and surface plasmon resonance utilizing metallic nanoparticles (*e.g.*, gold, silver, and aluminium) might augment the optical transition rate in the material owing to the increased creation of electron–hole pairs [7]. Silver and aluminium nanoparticles exert similar effects on the photocurrent of solar cells. The scattering-to-absorption ratio is augmented by increasing the nanoparticle size near the surface plasmon resonance. Researchers have demonstrated the capacity of nanoparticles to augment scattering, fluorescence, and emission [9, 10].

The concept of enhanced absorption by nanoparticles has been utilized in optoelectronic devices. The enhancement of the short-circuit current J_{sc} in *a*-Si:H solar cells was accomplished through the utilization of Au nanoparticles with diameters ranging from 50 to 100 nm. Numerous investigations have indicated that scattering effects prevail for large particle sizes (> 100 nm), but absorption effects dominate for smaller nanoparticles (< 50 nm), making this characteristic suitable for solar applications [11, 12]. Silver nanoparticles offer advanced solutions to enhance the efficiency of these cells due to their exceptional conductivity, effective light absorption, high sensitivity, resolution, and chemical stability. Metal nanoparticles (MNPs) have consistently attracted significant attention due to their substantial surface-to-volume ratio, plasmonic properties, and other related characteristics [13–15].

The adjustment of the surface plasmon resonance of the MNPs is extensively examined to investigate its practical uses in sensors, biodevices, data storage, spectroscopy methods, catalysis, solar cells, and more [16–19].

Different physical and chemical methods can synthesize Ag nanoparticles. The preparation of nanoparticles is an electrochemical deposition, vacuum deposition [20], chemical vapour deposition (CVD) [21], sol–gel technology [22], electrical deposition [23], and laser ablation [24, 25]. Laser ablation in liquid is a green method that is cheap and easy. Therefore, it is a good method for preparing Ag NPs with uniform size and shape. This work details the fabrication of Ag NPs using pulsed laser ablation in liquid at energies of 400 mJ and 1000 mJ in both water and acetone. It also assessed the

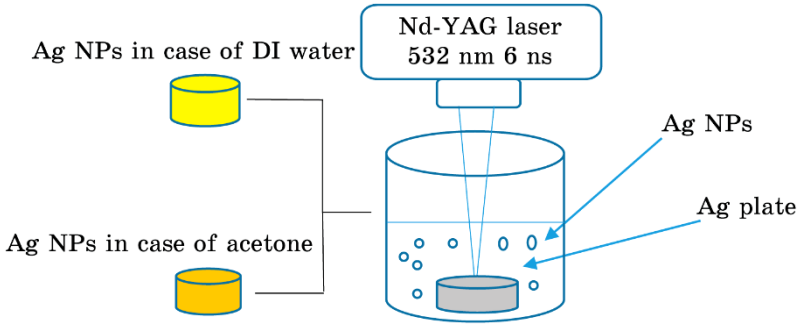

Fig. 1. Pulsed laser ablation in liquid technique.

influence of adding Ag NPs on silicon solar-cells' performance.

2. EXPERIMENTAL

First, silicon solar cells were subjected to hydrofluoric acid vapour for two minutes to remove the anti-reflective coating and any contamination on the front side of the silicon photovoltaic cells. The silicon solar-cell samples were immersed in deionized water (DIW) to eliminate the residual hydrofluoric acid. Secondly, silver colloid was synthesized *via* the pulsed laser-ablation technique (PLAL) at two energy levels 400 mJ and 1000 mJ, employing different solvents (deionized water and acetone), as illustrated in Fig. 1. Following preparation, the Ag NPs were applied to the surface of the silicon solar cell using the drop overcasting method, applying the Ag colloidal solution onto the heated surface of the solar cell and allowing it to dry [26].

Silver colloidal suspensions were characterized through optical absorption spectra recorded in the wavelength range of 320–1000 nm using a UV–Vis absorption spectrophotometer (model UV–Vis 721-2000), transmission electron microscopy (TEM), and photoluminescence spectroscopy.

3. RESULTS AND DISCUSSION

3.1. The Effect of Liquid

Figure 2 illustrates the TEM picture and the alteration in size of Ag NPs, when the laser was configured to 1000 mJ, with 700 pulses delivered at a repetition rate of 1 Hz. There was a 6 cm gap between the laser and target surfaces, and 7 cc of acetone and deionized water were utilized as fluids. The TEM picture indicates

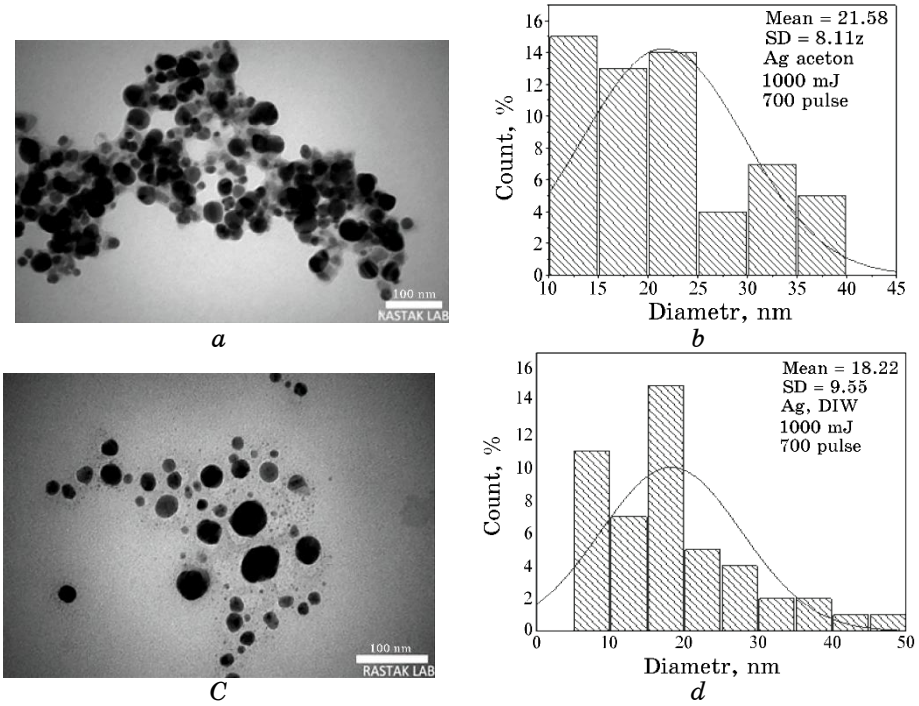

Fig. 2. The TEM image and the size distribution in percentage (histogram) of Ag NPs in acetone (*a*, *b*) and deionized water (*c*, *d*).

that the observed Ag NPs are mostly spherical across all mediums. No aggregation occurs in acetone; precipitation occurs, and the colloidal solution remains stable, as seen in Fig. 2, *a*. Particle sizes range from 10 nm to 40 nm. The particle size distribution is narrow, featuring a mean of 21.56 nm and a standard deviation of 8.11 nm, as illustrated in Fig. 2, *b*. Aggregation occurs in DIW due to the oxygen present, which triggers oxidation in the Ag NPs, as illustrated in Fig. 2, *c*. The figure demonstrates a remarkably limited size range particles ranging from 5 nm to 50 nm. A mean size of 18.22 nm and a standard variation of 9.55 nm are, as seen in Fig. 2, *d*.

Figure 3 illustrates the optical characteristics of silver nanoparticles synthesized in deionized water and acetone. The generated nanoparticles can be characterized by the emergence of SPR peaks in their corresponding spectra, which serve as markers of the particles' size and morphology. These obtained SPR peaks agreed with those reported in Refs. [27, 28]. We will witness an increase in absorption in DIW rather than acetone, owing to the increase in laser ablation efficiency that indicates an increase in the quantity of ab-

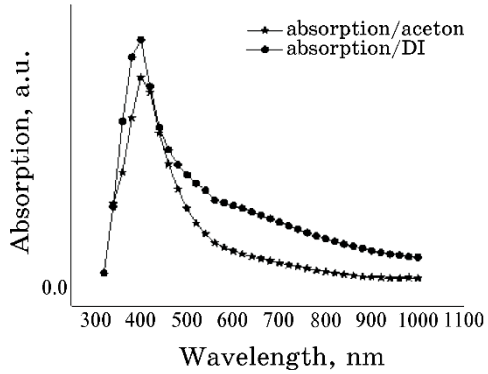

Fig. 3. Absorption of Ag NPs in acetone and DIW.

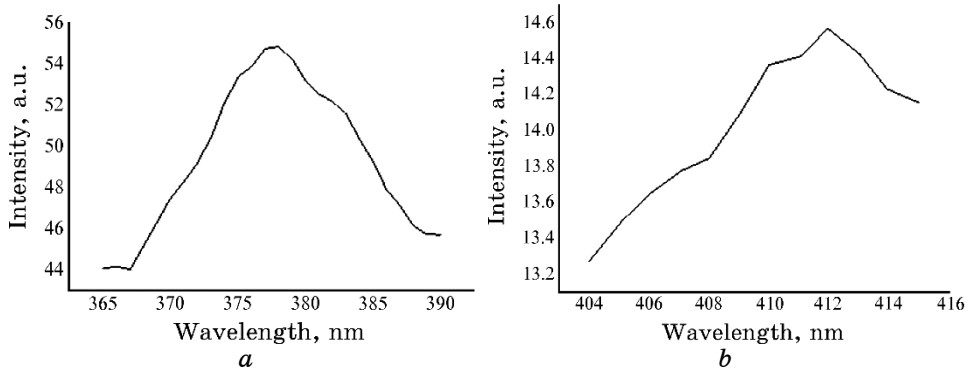

Fig. 4. PL spectroscopy of Ag NPs in different liquids: (*a*) acetone, (*b*) DIW.

lated material. At approximately 400 nm, the picture also reveals that the highest absorption occurs for Ag NPs. The spectra of the samples generated in DIW and acetone show peaks at 400 nm, which are attributed to the famous surface plasmon resonance of spherical particles [29].

Figure 4 illustrates the PL spectrophotometer results for Ag NPs in various liquids. It indicates that Ag NPs in acetone and deionized water exhibit photoluminescence emissions in the violet-blue and ultraviolet ranges. All particles exhibit a single emission peak at 378 nm for acetone and 412 nm for deionized water. As shown in Figure 5, which illustrates the band-structure excitation and recombination processes in noble metals [18, 30], the emission peaks at 378 nm and 412 nm denote the radiative recombination of electrons and holes moving from the *sp*-conduction band above the Fermi level to the *d*-band.

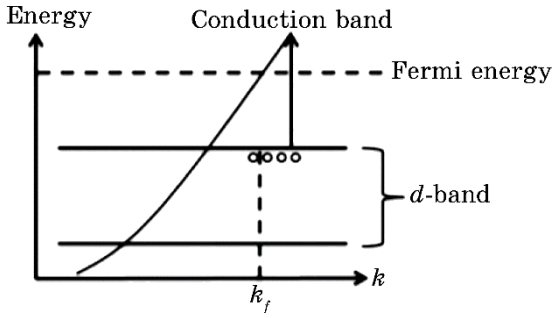

Fig. 5. The excitation and recombination mechanisms inside the band structure of noble metals.

As seen in Fig. 5, the band structure of noble metals, including silver (Ag), has a mechanism for excitation and recombination. The following procedures are depicted in the diagram.

1. Excitation. An electron is promoted from the lower energy *d*-band to the higher energy *sp*-band, when a silver nanoparticle absorbs a photon with enough energy. In the diagram, the ascending arrow represents this process.

2. Radiative recombination is the second process, and it involves the release of energy in the form of light (photoluminescence), when an excited electron recombines with a hole in the *d*-band. The diagrammatic descending arrow signifies this.

3. Surface Plasmon Resonance. The interaction of light with the free electrons in the *sp*-band leads to the generation of surface plasmon resonances, which are responsible for the enhanced optical properties of Ag NPs. The SPR effect is highly dependent on the size, shape, and dielectric environment of the nanoparticles.

The excitation and recombination mechanisms explain the photoluminescence (PL) peaks observed in the Ag NPs (*e.g.*, at 378 nm and 412 nm in acetone and DIW, respectively, as seen in Fig. 4). This mechanism is crucial for understanding how Ag NPs enhance light absorption and scattering in solar cells, leading to improved efficiency.

3.2. The Effect of the Energy

The TEM image and size distribution of Ag NPs at two energy levels (400 mJ, 1000 mJ), with 700 pulses and a repetition rate of 1 Hz, at a distance of 6 cm between the laser and target surfaces, using 7 ml of DIW, as seen in Fig. 6. DIW was chosen because the results showed that its absorption is better than that of acetone. As demonstrated at the energy of 400 mJ, the Ag NPs' size is modest

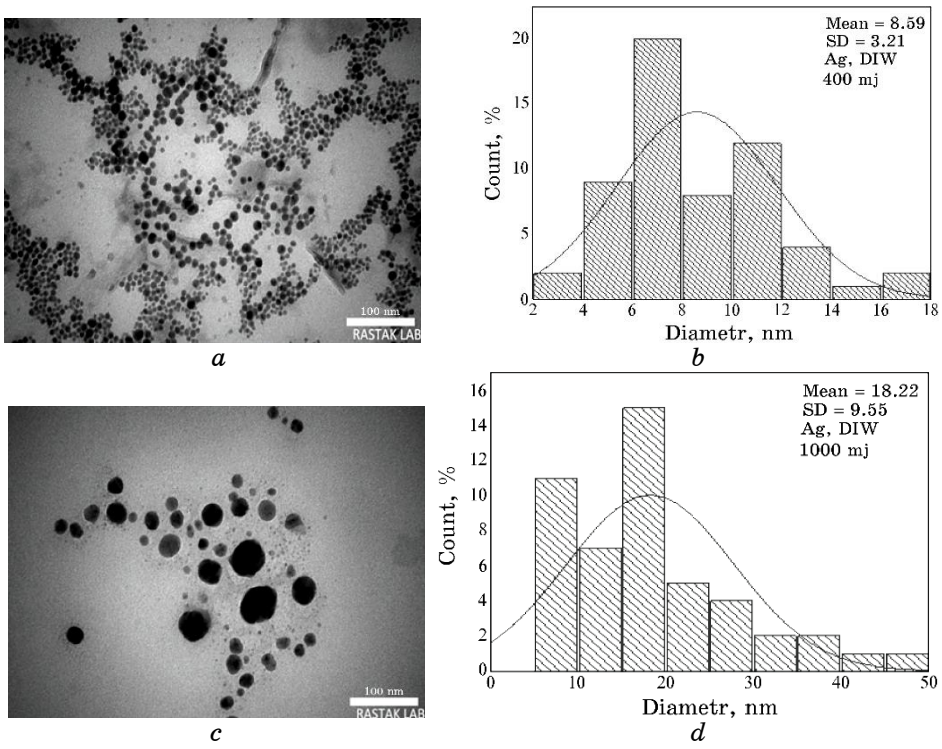

Fig. 6. The TEM image and the size distribution of Ag NPs at different energy: (*a*, *b*) 400 mJ, (*c*, *d*) 1000 mJ.

and uniform with spherical shape with range of 2–18 nm. The mean size is of 8.59 nm, and the standard deviation is of 3.2, as seen in Fig. 6, *a*, *b*. However, at energy 1000 mJ, the range is of 5–50 nm, the mean size is of 18.22, and the standard deviation is of 9.55, as seen in Fig. 6, *c* and *d*. Comparing the two energies, it is obvious that, with the lower energy, the particle size was smaller and homogeneous, and the number of particles was bigger compared to the higher energy, with a regular distribution. This is because the low-energy limits excessive evaporation. When the laser power is reduced, the amount of vaporized material is reduced, leading to the growth of small particles with a uniform distribution to avoid excessive evaporation and the formation of larger particles. With lower energy, cooling happens quicker in solution, favouring the production of tiny particles by restricting their development *via* fusion. Prevent particle accumulation: when the quantity of material generated is limited, the chance of collision between particles is lowered, preventing the production of bigger particles by chumping [31].

Figure 7 shows the optical properties of the Ag NPs in DI water at two energies of 400 mJ and 1000 mJ. As shown, the absorption at energy 1000 mJ is greater than at energy 400 mJ. Absorption peaks of Ag NPs may be changed at a given wavelength by variables dependent on the laser energy and the number of pulses. For optical absorbance of the colloidal solution, it has been shown that Ag NPs' exaction absorption peaks positioned at 400-mJ wavelength. An increase in the optical absorption with increased laser energy is owing to the growth in laser-ablation efficiency, which entails an increase for material. The absorption intensity rose by more than 80%, when the laser pulse energy was raised from 400 mJ to 1000 mJ.

The PL spectra of Ag NPs at 400 mJ and 1000 mJ in DI water are shown in Fig. 8. This figure shows that PL radiation is in the

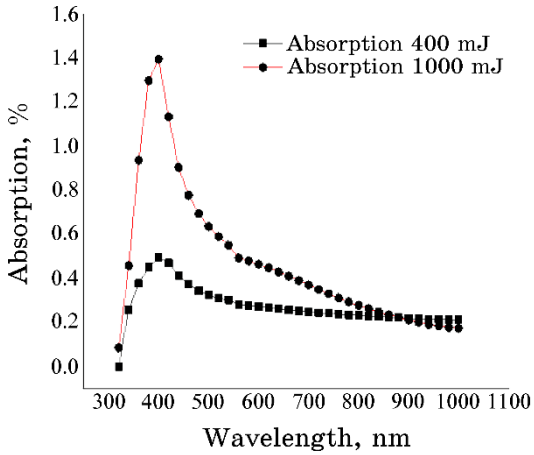

Fig. 7. UV–Vis spectrophotometry of Ag at different energy.

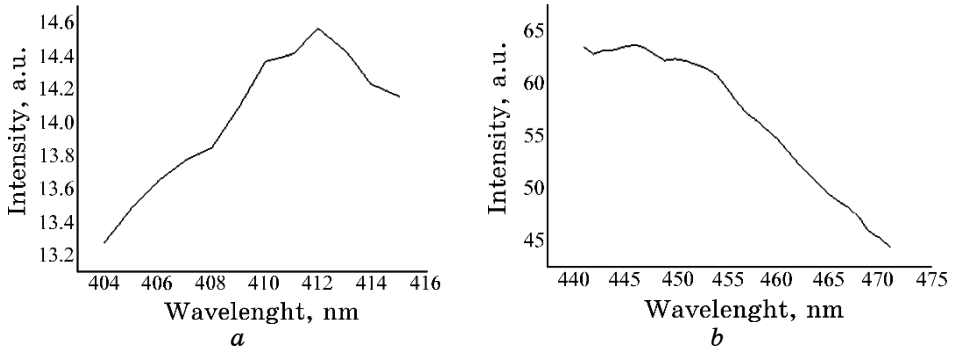

Fig. 8. PL spectrophotometry for Ag NPs at different energy: (*a*) 1000 mJ, (*b*) 400 mJ.

visible area, and there is one emission peak in PL for all particles found at 412 nm and 446 nm for 1000 mJ and 400 mJ, respectively. With the peak at 446 nm with strength of 63.6 a.u., silver nanoparticles exhibit distinctive photoluminescence properties, with the metallic solutions being stimulated at their corresponding plasmon absorption peaks [32]. The fluorescence originates from the excitation of *d*-band electrons in silver nanoparticles upon the absorption of incoming photon energy, elevating them to higher electronic states in the *sp*-band. The radiation at 412 nm and 446 nm is attributable to the surface plasmon resonance of Ag NPs [18, 33].

3.3. The Solar-Cell Result

Figure 9 illustrates the current–voltage (I–V) properties of silicon solar cells, both with and without Ag NPs. The I–V curve offers following essential metrics for assessing solar cell performance.

1. Short-Circuit Current (J_{sc}) is, when the voltage is zero. The addition of Ag NPs increases J_{sc} due to enhanced light absorption and reduced reflectivity.

2. Open-Circuit Voltage (V_{oc} is, when the current is zero. Ag NPs also improve V_{oc} by increasing the generation of electron–hole pairs.

3. Fill Factor (FF) is the ratio of the maximum power to the product of V_{oc} and J_{sc}. A higher FF indicates better solar-cell performance.

4. Power Conversion Efficiency (PCE) is the overall efficiency of the solar cell calculated from the I–V curve. The addition of Ag NPs increases PCE by nearly 20%.

The I–V curves demonstrate that the improvement in solar-cell performance is due to the plasmonic effects of Ag NPs.

The increase in J_{sc}, V_{oc}, and FF confirms that Ag NPs enhance light absorption and reduce energy losses in the solar cells.

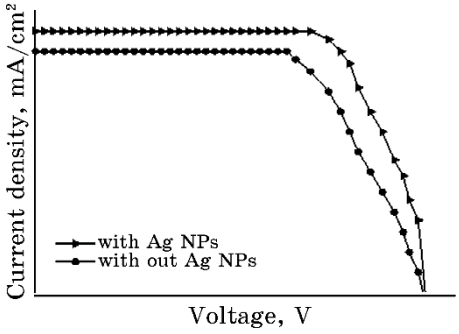

Fig. 9. The I–V characteristics of solar cells.

Table presents the solar-cell parameters in both the presence and the absence of Ag NPs. The rise in efficiency of the solar cell can be attributed to enhancements in the short-circuit current, open-circuit voltage, and fill factor; the most significant improvement was observed in the short-circuit current, which is linked to the increased plasmonic absorption of incident light resulting from the forward scattering of Ag NPs, thereby, decreasing reflectivity as illustrated in Fig. 10. The responsiveness of solar cells incorporating Ag NPs surpasses that of solar cells lacking Ag NPs. The data presented in Table and the I–V characteristics of solar cells illustrated in Fig. 9 indicate that the efficiency improved by nearly 20% with the incorporation of Ag NPs.

Figure 10 shows the reflectance spectra of a silicon wafer with Ag NPs.

1. Reduced Reflectance. The silicon wafer with Ag NPs exhibits lower reflectance across the visible spectrum compared to the wafer without Ag NPs. This is due to the forward scattering of light by the Ag NPs, which trap more light within the solar cell.

2. Enhanced Light Absorption. The reduction in reflectance leads to increased light absorption, which improves directly the solar-cells' efficiency.

3. Plasmonic Effects. The Ag NPs create localized surface plasmon resonance that enhances the electric field near the surface of the silicon wafer, further reducing reflectance and improving light trapping.

TABLE. Solar cell parameters without/with Ag NPs.

	J_{sc}, mA/cm^2	V_{oc}, V	FF	PCE, %
Without Ag NPs	5.204	0.625	0.652	2.121
With Ag NPs	6.019	0.667	0.687	2.756

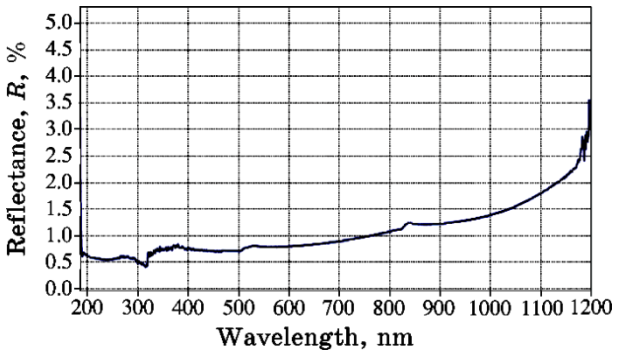

Fig. 10. The reflection of silicon wafer with Ag NPs.

The reflectance spectra confirm that Ag NPs reduce effectively the reflectivity of silicon solar cells, leading to enhanced light absorption and improved efficiency. This result supports the conclusion that Ag NPs are a promising solution for improving the performance of solar cells.

4. CONCLUSIONS

This work emphasized the synthesis of silver nanoparticles (Ag NPs) and the influence of laser energy and solvent on their creation. In addition, the effect of silver nanoparticles on the efficiency of the solar cell was studied. A pronounced surface plasmon resonance band was detected for Ag nanoparticles at 400 nm across several liquids (acetone, deionized water), exhibiting distinct absorption characteristics for each liquid. The absorption spectra of Ag NPs in acetone exceed those in deionized water. In deionized water, oxidation of the nanoparticles transpires, resulting in agglomeration within the colloidal solution, thus, diminishing absorbance. The analysis of several energy levels indicated that absorption increased by over 30% with rising laser energy. The deposition of Ag NPs on the front of the solar cell improved absorption in the visible spectrum, hence, increasing the solar cells' conversion efficiency by around 20% *via* surface plasmon resonance.

REFERENCES

1. S. Pillai and M. A. Green, *Sol. Energy Mater. Sol. Cells*, **94**: 1481 (2010); https://doi.org/10.1016/j.solmat.2010.02.046
2. Ji Hwang Lee, Jong Hwan Park, Jong Soo Kim, Dong Yun Lee, and Kilwon Cho, *Org. Electron.*, **10**, Iss. 3: 416 (2009); https://doi.org/10.1016/j.orgel.2009.01.004
3. Anamika Tewatia, Sarika Pal, and Narendra Pal, *Mater. Today Proc.*, **5**, Iss. 14, Pt. 2: 28384 (2018); https://doi.org/10.1016/j.matpr.2018.10.123
4. S. Venugopal Rao, G. Krishna Podagatlapalli, and Syed Hamad, *J. Nanosci. Nanotechnol.*, **14**, No. 2: 1364 (2014); https://doi.org/10.1166/jnn.2014.9138
5. Sri Priya Sundararajan, Nathaniel K. Grady, Nikolay Mirin, and Naomi J. Halas, *Nano Lett.*, **8**: 624 (2008); https://doi.org/10.1021/nl073030
6. Jinna He, Chunzhen Fan, Junqiao Wang, Yongguang Cheng, Pei Ding, and Erjun Liang, *Adv. Optoelectron*, **2012**: 592754 (2012); https://doi.org/10.1155/2012/592754
7. Ulrich W. Paetzold, Etienne Moulin, Bart E. Pieters, Uwe Rau, and Reinhard Carius, *J. Photonics Energy*, **2**: 027002 (2012); https://doi.org/10.1117/1.JPE.2.027002
8. Keisuke Nakayama, Katsuaki Tanabe, Harry A. Atwater, *Nanoscale Photonic Cell Technol. Photovoltaics*, **7047**: 704708 (2008);

https://doi.org/10.1117/12.795469
9. Mohammed Al-Azawi, Noriah Bidin, Abdulrahman Ali, Khaleel Hassoon, and Mundzir Abdullah, *Mod. Appl. Sci.*, **9**: 20 (2015); https://doi.org/10.5539/mas.v9n6p20
10. A. K. Ali and D. N. Raouf, *Eng. & Tech. Journal*, **29**: 15 (2011); https://pdfs.semanticscholar.org/0680/4631d9fc005d452eeea4aa1319053044ebdf.pdf
11. Hua-Min Li, Gang Zhang, Cheng Yang, Dae-Yeong Lee, Yeong-Dae Lim, Tian-Zi Shen, Won Jong Yoo, Young Jun Park, Hyunjin Kim, Seung Nam Cha, and Jong Min Kim, *J. Appl. Phys.*, **109**, Iss. 9: 093516 (2011); https://doi.org/10.1063/1.3587165
12. Hitomi Muto, Ken Miyajima, and Fumitaka Mafuné, *J. Phys. Chem. C*, **112**, Iss. 15: 5810 (2008); https://doi.org/10.1021/jp711353m
13. Paolo Prosposito, Federico Mochi, Erica Ciotta, Mauro Casalboni, Fabio De Matteis, Iole Venditti, Laura Fontana, Giovanna Testa, and Ilaria Fratoddi, *Beilstein J. Nanotechnol.*, **7**, 1654 (2016); https://doi.org/10.3762/bjnano.7.157
14. Siddhant Jain and Mohan Singh Mehata, *Sci. Rep.*, **7**: Article No. 15836 (2017); https://doi.org/10.1038/s41598-017-15724-8
15. Pragyan Roy, Bhagyalaxmi Das, Abhipsa Mohanty and Sujata Mohapatra, *Appl. Nanosci.*, **7**: 843 (2017); https://doi.org/10.1007/s13204-017-0621-8
16. Koppole Kamakshi, J. P. B. Silva, K. C. Sekhar, Gregory Marslin, J. Agostinho Moreira, O. Conde, A. Almeida, M. Pereira, and M. J. M. Gomes, *Appl. Phys. B: Lasers Opt.*, **122**: Article No. 123 (2016); https://doi.org/10.1007/s00340-016-6385-0
17. A. Serra, M. F. Cerqueira, D. P. Ferreira, and J. P. Borges, *Nanotechnology*, **20**, No. 16: 165501 (2009); https://doi.org/10.1088/0957-4484/20/16/165501
18. Koppole Kamakshi, J. P. B. Silva, K. C. Sekhar, J. Agostinho Moreira, A. Almeida, M. Pereira and M. J. M. Gomes, *Plasmonics*, **13**: 1235 (2018); https://doi.org/10.1007/s11468-017-0625-y
19. Koppole Kamakshi, K. C. Sekhar, A. Almeida, J. Agostinho Moreira, and M. J. M. Gomes, *J. Opt.*, **16**, No. 5: 055002 (2014); https://doi.org/10.1088/2040-8978/16/5/055002
20. R. N. Bhargava, D. Gallagher, X. Hong, and A. Nurmikko, *Phys. Rev. Lett.*, **72**, No. 3: 416 (1994); https://doi.10.1103/PhysRevLett.72.416
21. A. I. Dikusar, P. G. Globa, S. S. Belevskii and S. P. Sidel'nikova, *Surf. Eng. and App. Elec.*, **45**, No. 3: 171 (2009); https://doi.10.3103/S1068375509030016
22. Smita Gohil, Ramesh Chandra, Bhagyashree Chalke, Sangita Bose, and Pushan Ayyub, *Journ. of Nano. and Nanotec.*, **7**, No. 2: 641 (2007); https://doi.10.1166/jnn.2007.121
23. Sharad Kamble, Kaveri Bhosale, Mahesh Mohite, and Swapnali Navale, *Int. J. of Adv. Res. in Sci., Comm. and Tech.*, **3**, Iss. 7: 121 (2015); https://doi.10.48175/ijarsct-9485
24. Etsuko Sugawara and Hiroshi Nikaido, *Anti. Agents and Chemo*, **58**, Iss. 12: 7250 (2014); https://doi.10.1128/AAC.03728-14
25. Raad S. Sabry, Asaad M. Abbas, Firas S. Mohammed, and Wisam J. Aziz, *Jour. of Mat. Sci.: Mater. in Elect.*, **27**, Iss. 4: 3170 (2016);

https://doi.10.1007/s10854-015-4141-6
26. R. Fabbro, J. Fournier, P. Ballard, D. Devaux, and J. Virmont, *J. Appl. Phys.*, **68**: 775 (1990); https://doi.org/10.1063/1.346783
27. R. M. Tilaki, A. Irajizad, and S. M. Mahdavi, *Appl. Phys. A*, **84**: 215 (2006); https://doi.org/10.1007/s00339-006-3604-2
28. Young Hwan Kim, Don Keun Lee, and Young Soo Kang, *Colloids Surf. A: Physicochem. Eng. Asp.*, **257–258**: 273 (2005); https://doi.org/10.1016/j.colsurfa.2004.07.035
29. Young Hwan Kim, Don Keun Lee, and Young Soo Kang, *Colloids Surf. A: Physicochem. Eng. Asp.*, **257–258**: 273 (2005); https://doi.org/10.1016/j.colsurfa.2004.07.035
30. A. Pyatenko, K. Shimokawa, M. Yamaguchi, O. Nishimura, and M. Suzuki, *Appl. Phys. A: Mater. Sci. Process.*, **79**: 803 (2004); https://doi.org/10.1007/s00339-004-2841-5
31. R. Das, S. S. Nath, D. Chakdar, G. Gope, and R. Bhattacharjee, *J. Exp. Nanosci.*, **5**: 357 (2010); https://doi.org/10.1080/17458080903583915
32. Myungjoon Kim, Saho Osone, Taesung Kim, Hidenori Higashi, and Takafumi Seto, *KONA Powder Part. J.*, **34**: 80 (2017); https://doi.org/10.14356/kona.2017009
33. D. Ievlev, I. Rabin, W. Schulze, and G. Ertl, *Chem. Phys. Lett.*, **328**: 142 (2000); https://doi.org/10.1016/S0009-2614(00)00858-7
34. M. A. Garcia, *J. Phys. D: Appl. Phys.*, **44**: 283001 (2011); https://doi.org/10.1088/0022-3727/44/28/283001